

# Supporting Information

Perni et al. 10.1073/pnas.1610586114

## SI Materials and Methods

**Squalamine.** Squalamine (as the dilactate salt) was synthesized as previously described (49) and was greater than 97% pure.

### Experiments with DOPS:DOPE:DOPC Vesicles.

**Protein expression and purification.** N-terminally acetylated  $\alpha$ -synuclein, which is the most prevalent form of  $\alpha$ -synuclein in mammalian cells and also increases membrane affinity (45–47), was obtained as previously described (45). Briefly, N-terminal acetylation of WT  $\alpha$ -synuclein was achieved by coexpression of a plasmid carrying the components of the NatB complex with a plasmid containing the wild-type  $\alpha$ -synuclein gene, following the protocol described previously (48). We observed that the restrictive conditions of M9 media have a strong effect on the acetylation reaction. Essentially complete acetylation ( $\geq 98\%$ ) was observed only when using protonated M9 medium, supplemented with 1 g/L protonated IsoGro (Sigma). Unless noted otherwise, all NMR experiments with acetylated  $\alpha$ -synuclein were performed on  $^{15}\text{N}$ - and  $^{13}\text{C}$ -labeled  $\alpha$ -synuclein samples, obtained using [ $^{15}\text{N}$ ,  $^{13}\text{C}$ ] IsoGro.

**Preparation of vesicles.** Phospholipids were purchased from Avanti Polar Lipids as a lyophilized powder of a DOPE/DOPS/DOPC mixture with a 5:3:2 weight ratio (coagulation reagent I). Vesicles were prepared as described previously (27) in 20 mM imidazole buffer [pH 6, 10% (wt/vol)].

**NMR spectroscopy.** NMR experiments were performed using a 600-MHz Bruker spectrometer equipped with a cryoprobe. The sample temperature was set to 288 K, and the sample buffer composition was 20 mM imidazole, 100 mM NaCl, pH 6. Squalamine is highly soluble in distilled water, but its solubility in 20 mM imidazole, 100 mM NaCl is reduced to ca. 130  $\mu\text{M}$ . Concentrations above this level result in NMR-invisible, light-scattering aggregates. The solubility in PBS (pH 7.4) solution was measured at ca. 35  $\mu\text{M}$ .

**CD Spectroscopy.** All CD measurements were taken at 20  $^\circ\text{C}$ , using a 1-mm path-length cuvette. Samples contained 20 mM Tris (pH 7.4), 100 mM NaCl, 5  $\mu\text{M}$  N-terminally acetylated  $\alpha$ -synuclein, and 0.1% wt/vol lipid vesicles (ca. 1.25 mM). The vesicles consisted of 30% DOPS, 50% DOPE, and 20% DOPC.

### Experiments with DMPS Vesicles.

**Reagents.** Sodium salt (DMPS) was purchased from Avanti Polar Lipids. Sodium phosphate monobasic ( $\text{NaH}_2\text{PO}_4$ ; BioPerformance certified,  $\geq 99.0\%$ ), sodium phosphate dibasic ( $\text{Na}_2\text{HPO}_4$ ; Reagent-Plus,  $\geq 99.0\%$ ), sodium chloride (NaCl; BioXtra,  $\geq 99.5\%$ ), and sodium azide ( $\text{NaN}_3$ ; ReagentPlus,  $\geq 99.5\%$ ) were purchased from Sigma Aldrich. ThT UltraPure Grade ( $\geq 95\%$ ) was purchased from Eurogentec.

**Protein expression and lipid preparation.** WT (nonacetylated)  $\alpha$ -synuclein was expressed in *E. coli* and purified as previously described (10, 50). The lipids were dissolved in 20 mM phosphate buffer ( $\text{NaH}_2\text{PO}_4/\text{Na}_2\text{HPO}_4$ ) (pH 6.5), 0.01%  $\text{NaN}_3$  and stirred at 45  $^\circ\text{C}$  for 2 h. The solution was then frozen and thawed five times, using dry ice and a water bath at 45  $^\circ\text{C}$ . The preparation of vesicles was carried out using sonication (Bandelin Sonopuls HD 2070, 3  $\times$  5 min, 50% cycles, 10% maximum power) on ice. After centrifugation, the sizes of the vesicles were checked using dynamic light scattering (Zetasizer Nano ZSP; Malvern Instruments) and were shown to consist of a distribution centered at a diameter of 20 nm.

### CD spectroscopy.

**Data acquisition.** CD samples were prepared as previously described (12) by incubating 20  $\mu\text{M}$   $\alpha$ -synuclein in the presence of 1 mM DMPS vesicles in 20 mM phosphate buffer (pH 6.5), 0.01%  $\text{NaN}_3$ , and increasing concentrations of squalamine. A squalamine stock solution was prepared by dissolving the molecule in doubly distilled water to a final concentration of 5 mM. Far-UV CD spectra were recorded on a JASCO J-810 instrument equipped with a Peltier thermally controlled cuvette holder at 30  $^\circ\text{C}$ . Quartz cuvettes with path lengths of 1 mm were used, and CD spectra were obtained by averaging five individual spectra recorded between 250 nm and 200 nm with a bandwidth of 1 nm, a data pitch of 0.2 nm, a scanning speed of 50 nm/min, and a response time of 1 s. Each value of the CD signal intensity reported at 222 nm corresponds to the average of three measurements, each acquired for 10 s. For each protein sample, the CD signal of the buffer used to solubilize the protein was recorded and subtracted from the CD signal of the protein.

**Data analysis.** The change in the concentration of  $\alpha$ -synuclein bound to the DMPS vesicles with increasing concentration of squalamine was fitted to the same competitive binding model as the one described for the competitive binding of  $\alpha$ -synuclein and  $\beta$ -synuclein to DMPS vesicles (22), taking into account the different stoichiometries in which DMPS binds to  $\alpha$ -synuclein and squalamine. The equations for the binding equilibria are

$$K_{D,\alpha} = \frac{[DMPS_f][\alpha_f]}{L_\alpha[\alpha_b]} \quad [S1]$$

$$K_{D,S} = \frac{[DMPS_f][S_f]}{L_S[S_b]} \quad [S2]$$

where  $K_{D,\alpha}$  and  $K_{D,S}$  are the binding constants of  $\alpha$ -synuclein and squalamine, respectively;  $[\alpha_f]$  and  $[\alpha_b]$  are the concentrations of free and bound  $\alpha$ -synuclein;  $[S_f]$  and  $[S_b]$  are the concentrations of free and bound squalamine;  $[DMPS_f]$  is the concentration of free DMPS; and  $L_\alpha$  and  $L_S$  denote the stoichiometries in which DMPS binds to  $\alpha$ -synuclein and squalamine, i.e., the number of molecule of DMPS interacting with one molecule of either  $\alpha$ -synuclein or squalamine, respectively.

By using the mass conservation equations,

$$[\alpha] = [\alpha_b] + [\alpha_f] \quad [S3]$$

$$[S] = [S_b] + [S_f] \quad [S4]$$

$$[DMPS] = [DMPS_f] + L_S[S_b] + L_\alpha[\alpha_b], \quad [S5]$$

where  $[\alpha]$ ,  $[S]$ , and  $[DMPS]$  are the total concentrations of  $\alpha$ -synuclein, squalamine, and DMPS, respectively. An expression for  $[\alpha_b]$  in terms of  $K_{D,\alpha}$ ,  $K_{D,S}$ ,  $L_\alpha$ ,  $L_S$ ,  $[\alpha]$ ,  $[S]$ , and  $[DMPS]$  can be derived. This is the standard solution of the cubic equation:

$$K_{D,\alpha} = \frac{([DMPS] - L_S[S_b] - L_\alpha[\alpha_b])([\alpha] - [\alpha_b])}{L_\alpha[\alpha_b]} \quad [S6]$$

$$[S_b] = \frac{[DMPS] - L_\alpha[\alpha_b] + K_{D,S}L_S + L_S[S]}{2L_S}$$

$$\sqrt{\frac{4L_S([\alpha_b]L_\alpha[S] - [DMPS][S]) + ([DMPS] - [\alpha_b]L_\alpha + K_{D,S}L_S + L_S[S])^2}{2L_S}} \quad [S7]$$

Its solution is not shown here due to its length. For each data point, the concentrations  $[\alpha_b]$ ,  $[S]$ , and  $[DMPS]$  are known, and the equilibrium constant and stoichiometry for the  $\alpha$ -synuclein/DMPS system,  $K_{D,\alpha}$  and  $L_\alpha$ , were set to the values determined previously (12). The variation of  $[\alpha_b]$  at a fixed  $[DMPS]$  (1 mM) and  $[S]$  (20  $\mu$ M), with increasing  $[S]$ , was fitted using the resulting equation with two unknowns,  $K_{D,S}$  and  $L_S$ , and the best fit is obtained for  $K_{D,S} = 67$  nM and  $L_S = 7.4$  (Fig. 3B).

#### Aggregation kinetics.

**Sample preparation and data acquisition.**  $\alpha$ -Synuclein was incubated in 20 mM sodium phosphate (pH 6.5), 0.01%  $\text{NaN}_3$ , in the presence of 50  $\mu$ M ultrapure ThT, 100  $\mu$ M DMPS vesicles, and increasing concentrations of squalamine (0–10  $\mu$ M). The stock solution of squalamine was prepared by dissolving the molecule in 20 mM phosphate buffer to a final concentration of 100  $\mu$ M. The change in the ThT fluorescence signal with time was monitored using a plate reader (BMG Labtech) under quiescent conditions at 30  $^\circ\text{C}$ . Corning 96-well plates with half-area (black/clear bottom polystyrene) nonbinding surfaces were used for each experiment. The data were then analyzed as described previously (12).

**Data analysis.** To determine the rate of lipid-induced aggregation of  $\alpha$ -synuclein at different squalamine concentrations, we used the same model as the one describing the inhibition of  $\alpha$ -synuclein lipid-induced aggregation by  $\beta$ -synuclein (22): The rate depends on the fractional coverage of a lipid vesicle in  $\alpha$ -synuclein ( $\theta_\alpha$ ) and we define  $n_b$  as the reaction order with respect to  $\theta_\alpha$ . We can adapt the equations given in ref. 12 to reflect this,

$$M(t) = \frac{K_M k_+ m(0)^{n+1} k_n [DMPS] \theta_\alpha^{n_b} t^2}{2(K_M + m(0))L_\alpha} \quad [S8]$$

where  $t$  is the time,  $M(t)$  is the aggregate mass,  $m(0)$  is the free monomer concentration,  $K_M$  is the saturation constant of the elongation process,  $k_n$  and  $k_+$  are the rate constants of nucleation and elongation, respectively, and  $\frac{[DMPS]}{L_\alpha}$  is the concentration of protein-binding sites at the surface of the membrane. We initially used Eq. S8 to fit the early times of the kinetic traces measured for  $\alpha$ -synuclein in the presence of 100  $\mu$ M DMPS and in the absence of squalamine (where  $\theta_\alpha = 1$  as we are in a regime where the vesicles are saturated), with  $K_M$ ,  $k_n k_+$ , and  $n$  being global fitting parameters (fit, Fig. 3B). The global fit yields  $n = 0.624$ ,  $K_M = 54$   $\mu$ M, and  $k_n k_+ = 9.9 \times 10^{-3} \text{ M}^{-(n+1)} \text{ s}^{-2}$ . The values obtained for these three parameters were then used as inputs into the fitting of the data in the presence of squalamine. The assumption that the presence of squalamine merely alters the fraction of  $\alpha$ -synuclein bound but does not affect any of the other rates is implicit. We then fitted the data in the presence of squalamine, with all parameters fixed to their values in the absence of squalamine, with the exception of  $\theta_\alpha^{n_b}$ . All fits were within error of the experimental data. This way we obtain  $\theta_\alpha^{n_b}$  at all  $\alpha$ -synuclein and squalamine concentrations.

We then used a simplified competitive binding model to analyze the change of  $\theta_\alpha^{n_b}$  with changing squalamine: $\alpha$ -synuclein ratios, to determine  $n_b$ . In the competitive binding model described above, the solution to Eq. S6 simplifies when all binding

sites on the vesicles can be assumed to be occupied, as is the case in the kinetic experiments. In this case Eq. S5 becomes  $[DMPS] \approx L_S[S_b] + L_\alpha[\alpha_b]$ . The concentration of bound  $\alpha$ -synuclein is then simply given by

$$[\alpha_b] = \frac{[DMPS]L_\alpha\kappa - [DMPS]L_S - [\alpha]L_\alpha L_S - L_\alpha L_S[S]\kappa}{2(L_\alpha^2\kappa - L_\alpha L_S)} + \frac{\sqrt{4[\alpha][DMPS]L_S(L_\alpha^2\kappa - L_\alpha L_S) + \left([DMPS]L_S + [\alpha]L_\alpha L_S - [DMPS]L_\alpha\kappa + L_\alpha L_S[S]\kappa\right)^2}}{2(L_\alpha^2\kappa - L_\alpha L_S)} \quad [S9]$$

where  $\kappa = \frac{K_{D,\alpha}}{K_{D,S}}$ . The global fits of  $\theta_\alpha^{n_b} = \left(\frac{[\alpha_b]L_\alpha}{[DMPS]}\right)^{n_b}$  agree well with the data (Fig. 3D) and we obtain  $n_b = 5.5$ .

#### Mass Spectrometry Experiments on $\alpha$ -Synuclein and A $\beta$ Fibrils.

**Preparation of fibrils.**  $\alpha$ -Synuclein fibrils were prepared as described previously (10, 51). Briefly, a 500- $\mu$ L sample of  $\alpha$ -synuclein at a concentration of 600  $\mu$ M was incubated in 20 mM phosphate buffer (pH 6.5) for 72 h at about 40  $^\circ\text{C}$  and stirred at 1,500 rpm with a Teflon bar on an RCT Basic Heat Plate (IKA). Fibrils were diluted to a monomer equivalent concentration of 200  $\mu$ M, divided into aliquots, flash frozen in liquid  $\text{N}_2$ , and stored at  $-80$   $^\circ\text{C}$  for experiments. For experiments with the A $\beta$  peptide (in this work we used the 42-residue form), fibrils were prepared as described previously (13). Briefly, A $\beta$  monomer at a concentration of 78  $\mu$ L was incubated in 20 mM phosphate buffer (pH 8) with 200  $\mu$ M EDTA, 0.02%  $\text{NaN}_3$ , for 6 h at about 37  $^\circ\text{C}$ . Before mass spectrometry analysis, 78  $\mu$ M of equivalent  $\alpha$ -synuclein and A $\beta$  fibrils was centrifuged at 100,000  $\times g$  for 1 h at the ultracentrifuge. The pellet was then resuspended in the same volume of Tris buffer for further analysis.

**Preparation of samples for mass spectrometry experiments.** Fibrils of  $\alpha$ -synuclein or A $\beta$  at a concentration of 10  $\mu$ M were incubated with 10  $\mu$ M squalamine in 20 mM Tris (pH 7.4), 100 mM NaCl overnight under quiescent conditions at room temperature. The samples were afterward centrifuged at 100,000  $\times g$  for 30 min at the ultracentrifuge. The supernatant was then removed for analysis. In the present work the experiments were run using a Waters Corporation Xevo G2-S QTOF.

#### Experiments on Human SH-SY5Y Neuroblastoma Cells.

**Preparation of oligomers.** Samples enriched in oligomeric  $\alpha$ -synuclein species were prepared as previously described (34). Briefly, monomeric  $\alpha$ -synuclein was lyophilized in Milli-Q water and subsequently resuspended in PBS, pH 7.4, to give a final concentration of ca. 800  $\mu$ M (12 mg/mL). The resulting solution was passed through a 0.22- $\mu$ m cutoff filter before incubation at 37  $^\circ\text{C}$  for 20–24 h under quiescent conditions. Very small amounts of fibrillar species formed during this time were removed by ultracentrifugation for 1 h at 90,000 rpm (using a TLA-120.2 Beckman rotor, 288,000  $\times g$ ). The excess monomeric protein and some small oligomers were then removed by multiple filtration steps, using 100-kDa cutoff membranes. The final concentration of oligomers was estimated based on the absorbance at 275 nm, using a molar extinction coefficient of 5,600  $\text{M}^{-1}\text{cm}^{-1}$ .

**Neuroblastoma cell culture.** Human SH-SY5Y neuroblastoma cells (A.T.C.C.) were cultured in DMEM, F-12 HAM with 25 mM Hepes and  $\text{NaHCO}_3$  (1:1) and supplemented with 10% FBS, 1 mM glutamine, and 1.0% antibiotics. Cell cultures were maintained in a 5%  $\text{CO}_2$  humidified atmosphere at 37  $^\circ\text{C}$  and grown until they reached 80% confluence for a maximum of 20 passages (24).

**MTT reduction assay.**  $\alpha$ -Synuclein oligomers (24) (0.3  $\mu$ M) were incubated with or without increasing concentrations (0.03  $\mu$ M,

0.1  $\mu\text{M}$ , 0.3  $\mu\text{M}$ , 1  $\mu\text{M}$ , and 3  $\mu\text{M}$ ) of squalamine for 1 h at 37 °C under shaking conditions and then added to the cell culture medium of SH-SY5Y cells seeded in 96-well plates for 24 h. The protein:squalamine molar ratios used here were 10:1, 3:1, 1:1, 1:3, and 1:10. The MTT reduction assay was performed as previously described (43).

**Measurement of intracellular ROS.**  $\alpha$ -Synuclein oligomers (0.3  $\mu\text{M}$ ) were preincubated for 1 h with or without increasing concentrations (0.03  $\mu\text{M}$ , 0.3  $\mu\text{M}$ , and 3  $\mu\text{M}$ ) of squalamine for 1 h at 37 °C under shaking and then added to the cell culture medium of SH-SY5Y cells seeded on glass coverslips for 15 min. To detect intracellular ROS production, cells were then loaded with 10  $\mu\text{M}$  CM-H<sub>2</sub>DCFDA (Life Technologies) as previously described (43). Cell fluorescence was analyzed by a TCS SP5 scanning confocal microscopy system (Leica Microsystems) equipped with an argon laser source, using the 488-nm excitation line. A series of 1.0- $\mu\text{m}$ -thick optical sections (1,024  $\times$  1,024 pixels) was taken through the cells for each sample, using a Leica Plan Apo 63 oil immersion objective, and then projected as a single composite image by superimposition. The confocal microscope was set at optimal acquisition conditions, e.g., pinhole diameters, detector gain, and laser powers. Settings were maintained constant for each analysis.

**Oligomer binding to the cellular membrane.** SH-SY5Y cells were seeded on glass coverslips and treated for 15 min with  $\alpha$ -synuclein oligomers (0.3  $\mu\text{M}$ ) and increasing concentrations (0.03  $\mu\text{M}$ , 0.1  $\mu\text{M}$ , 0.3  $\mu\text{M}$ , 1  $\mu\text{M}$ , and 3  $\mu\text{M}$ ) of squalamine. After incubation, the cells were washed with PBS and counterstained with 5.0  $\mu\text{g}/\text{mL}$  Alexa Fluor 633-conjugated wheat-germ agglutinin (Life Technologies). After washing with PBS, the presence of oligomers was detected with 1:250 diluted rabbit polyclonal anti- $\alpha$ -synuclein antibodies (Abcam) and subsequently with 1:1,000 diluted Alexa Fluor 488-conjugated anti-rabbit secondary antibodies (Life Technologies). Fluorescence emission was detected after double excitation at 488 nm and 633 nm by the scanning confocal microscopy system described above and three apical sections were projected as a single composite image by superimposition.

### **C. elegans Experiments.**

**Media.** Standard conditions were used for the propagation of *C. elegans* (52). Briefly, the animals were synchronized by hypochlorite bleaching, hatched overnight in M9 (3 g/L KH<sub>2</sub>PO<sub>4</sub>, 6 g/L Na<sub>2</sub>HPO<sub>4</sub>, 5 g/L NaCl, 1 M MgSO<sub>4</sub>) buffer, and subsequently cultured at 20 °C on nematode growth medium (NGM) [1 mM CaCl<sub>2</sub>, 1 mM MgSO<sub>4</sub>, 5  $\mu\text{g}/\text{mL}$  cholesterol, 250 M KH<sub>2</sub>PO<sub>4</sub> (pH 6), 17 g/L Agar, 3 g/L NaCl, 7.5 g/L casein] plates seeded with the *E. coli* strain OP50. Saturated cultures of OP50 were grown by inoculating 50 mL of LB medium (10 g/L tryptone, 10 g/L NaCl, 5 g/L yeast extract) with OP50 and incubating the culture for 16 h at 37 °C. NGM plates were seeded with bacteria by adding 350  $\mu\text{L}$  of saturated OP50 to each plate and leaving the plates at 20 °C for 2–3 d. On day 3 after synchronization, the animals were placed on NGM plates containing 5-fluoro-2'-deoxy-uridine (FUDR) (75  $\mu\text{M}$ , unless stated otherwise) to inhibit the growth of offspring.

**Strains.** The following strains were used. zgIs15 [P(unc-54):: $\alpha$ syn::YFP]IV (OW40): In OW40,  $\alpha$ -synuclein fused to YFP relocates to inclusions, which are visible as early as day 2 after hatching and increase in number and size during the aging of the animals, up to late adulthood (day 17) (25). rmIs126 [P(unc-54)Q0::YFP]V (OW450): In OW450, YFP alone is expressed and remains diffusely localized throughout aging (25). dvIs2 [pCCL12(unc-54/human A $\beta$  1–42 peptide minigene) + pRF4]: Where A $\beta$ <sub>42</sub> aggregates giving rise to adult onset paralysis and egg-laying, deficiency is observed when the temperature is raised to 20 °C.

**Squalamine administration.** Aliquots of NGM media containing FUDR (75  $\mu\text{M}$ ) were autoclaved, poured, seeded with 350  $\mu\text{L}$

OP50 culture, and grown overnight. After incubating for up to 3 d at room temperature, 2.2-mL aliquots of squalamine dissolved in water at different concentrations were spotted atop the NGM plates. The plates were then placed in a sterile laminar flow hood at room temperature to dry. We first observed that the compound was toxic when administered to the worms from L1 larval stage (25% worm death), probably due to the high membrane permeability of the worms in this stage. For the final experiments, worms were transferred onto the squalamine-seeded plates directly at larval stage L4 and they were exposed to squalamine for the whole duration of the experiment.

**Thrashing assays.** At different ages, animals were placed in a drop of M9 buffer and allowed to recover for 30 s (to avoid observing behavior associated with stress) after which the number of body bends was counted for either 30 s or 1 min. For blinded motility assays, adult animals were randomly picked from the treated and untreated populations and measured for motility without knowledge of the squalamine concentration. Thirty animals were counted in each experiment unless stated otherwise. Experiments were carried out in triplicate and the data from one representative experiment are shown in Fig. S4. Statistical analysis was performed using Graphpad Prism software (GraphPad Software) (37).

**Automated motility assay.** All *C. elegans* populations were cultured at 20 °C and developmentally synchronized from a 4-h egg lay. At 64–72 h post-egg lay (time 0) individuals were transferred to FUDR plates or into multiwells and body movements were assessed over the times indicated. For experiments carried out on agar plates, at different ages, the animals were washed off the plates with M9 buffer and spread over an OP50 unseeded 6-cm plate, after which their movements were recorded at 30 fps, using a novel microscopic setup for 30 s or 1 min. For screenings in multiwells, worms were mixed on a bench-top plate shaker at 700 rpm for 7 min to evenly distribute sedimented OP50 and induce full worm motility. Immediately after shaking, worms were staged on the platform for imaging. File collection was initiated 60 s after shaking. Up to 200 animals were counted in each experiment unless stated otherwise. One experiment that is representative of the three measured is shown in Fig. 5. Movies were analyzed using a custom-made tracking code.

**Paralysis assays.** Paralysis assays were performed by transferring L4 larvae synchronized animals to NGM plates and they were grown at 15 °C until the first day of adulthood (2 d after L4) to avoid developmental defects of the vulva. The L4 larvae or the young adult animals were transferred to squalamine plates containing FUDR and the temperature was raised to 20 °C. Each individual experiment was initiated with 100 L4 or young adult animals per strain. The animals were tested for paralysis by tapping their noses and tails, prodding with a platinum wire as described previously (53) every day for 14 consecutive days. Worms that moved their noses but failed to move their bodies were scored as paralyzed. Data from one representative of three experiments are shown in Fig. S5. Analysis was performed using Graphpad Prism software (GraphPad Software) (37).

**Quantification of inclusions.** To monitor the number of inclusions in each worm, individual animals were mounted on 2% agarose pads, containing 40 mM NaN<sub>3</sub> as an anesthetic, on glass microscope slides for imaging. For quantification of the number of inclusions in  $\alpha$ -synuclein:YFP animals, only the frontal region of the worms was considered (25). The number of inclusions in each animal was quantified using a Leica MZ16 FA fluorescence dissection stereomicroscope (Leica Microsystems) at a nominal magnification of 20 $\times$  or 40 $\times$ , and images were acquired using an Evolve512 Delta EMCCD camera, with high quantum efficiency (Photometrics). Measurements on inclusions were performed using ImageJ software (54) (National Institutes of Health). At least 50 animals were examined per condition, unless stated otherwise. All experiments were carried out in triplicate and the data from one representative experiment are shown in Figs. 4

and 5. Student's *t* test was used to calculate *P* values, and all tests were two-tailed unpaired unless otherwise stated.

**Western blot analysis.** For comparison of  $\alpha$ -synuclein levels, ca. 3,000 adults were collected in S-basal (52) in triplicate and then frozen in liquid N<sub>2</sub>. Samples were then extracted in Urea/SDS buffer (8 M urea, 2% SDS, 50 mM Tris, 1 $\times$  proteinase inhibitors) (Roche Holding) and disrupted via sonication. Samples at the appropriate concentration were added to NuPAGE LDS Sample Buffer (1 $\times$ ) and NuPAGE Sample Reducing Agent (1 $\times$ ) (Life Technologies) and heated at 70 °C for 10 min. The material was resolved via NuPAGE Novex 4–12% Bis-Tris Protein Gels (Life Technologies) and then transferred to nitrocellulose membranes, using an iBlot Dry Blotting System (Life Technologies), and blocked overnight at 4 °C in 5% BSA. Membranes were then probed at room temperature with SYN-1 anti- $\alpha$ -synuclein antibody, clone 42 (BD Biosciences) 1:500. Anti- $\alpha$ -tubulin, clone B-5-1-2 (Sigma-Aldrich) 1:10,000, was used to standardize total protein loading. An Alexa 488-conjugated secondary antibody, A11029 (Life Technologies), was used for detection.

### SI Text

**Automated Motility Assay.** We built a simple, robust, compact, cost-effective and high-throughput setup to track *C. elegans* during swimming and crawling. An LED backlight illuminator with long life span and flicker-free and shadow-free illumination was used to illuminate worms moving in M9 buffer on a thin agar plate or in multiwells. The swimming worms were visualized by using a high-performance imaging lens and a machine vision camera. The movies of the swimming worms were taken at a high number of fps for 30 s or 1 min. Different fields of view were obtained simply by changing the distance between the sample and the lens, for a fixed focal length of the lens and camera sensor size. Using this setup we were able to image successfully at the same time up to 200 swimming animals over the whole surface of a 6-cm agar plate or inside multiwells.

To analyze the worm movement from the movies, the first step was to detect and subtract the background. If all worms are alive, this procedure can be carried out by temporally averaging the movies. If some of the worms are dead, however, this method will skew the final statistics because the dead worms will be taken as part of the background and thus not be included in the signal. This is particularly important for high-throughput testing of drugs, because certain drugs might influence the life-to-death ratio and paralysis rate. Thus, the background must be estimated without using temporal information. In our method we begin by defining a Gaussian adaptive threshold of the image in such a way that all worms are identified. Such a threshold that ensures detection of

all worms will also incorrectly elaborate some of the background signal as worms and so is not a completely reliable detection mechanism in itself. All pixels marked as worms are then recalculated by interpolating from pixels not marked as worms. This procedure avoids removing the dead worms as part of the background. The method requires the movie to be quite regular, however, and hence other items, such as the edge of a Petri dish, must first be masked by other methods. After background subtraction a second (nonadaptive) thresholding procedure is performed. Morphological operations are next used to remove speckles (morphological opening) and to close holes that can appear in the worms after the thresholding (morphological closing). We label all separated regions of the thresholded image and remove all regions that have an area too small or big to be a single worm. The remaining labeled regions are identified as individual worms. The positions of said regions are then stored for each frame. Subsequently these regions are linked across the frames by standard tracking algorithms, even taking into account a worm disappearing or overlapping in a few frames. The eccentricity, a measure of the ratio of the minor and major ellipse axes, of each tracked worm can then be used to estimate the worm bending as a function of time.

**Detection of the Interaction of Squalamine with Monomeric  $\alpha$ -Synuclein at High Concentrations in the Absence of Lipids.** The changes in the NMR spectrum indicate that the  $\alpha$ -synuclein–squalamine interaction is in the fast exchange regime, as the residues of  $\alpha$ -synuclein that are affected by the binding progressively shift their resonance positions as the concentration of squalamine is increased; as a consequence of the broadening a loss of intensity is also observed (Fig. S1). An indication that the interaction involves an aggregated state of squalamine comes from the observation that at a high squalamine concentration some of the C-terminal residues of  $\alpha$ -synuclein (e.g., Y136) experience a large degree of line broadening despite showing only modest changes in chemical shifts. Resonance broadening is likely to result from two factors: a chemical exchange contribution, caused by perturbations in chemical shifts, and an increase in the dipolar contribution to the transverse relaxation rate, R<sub>2</sub>, caused by the increased size of the complex. Considering that the chemical shift change for Y136 is small, the R<sub>2</sub> contribution must dominate, suggesting that the complex is significantly larger in size than the monomer. This finding is consistent with the involvement of multimeric squalamine in the interaction, analogous to the interaction between  $\alpha$ -synuclein and micellar Congo Red (CR) (55).

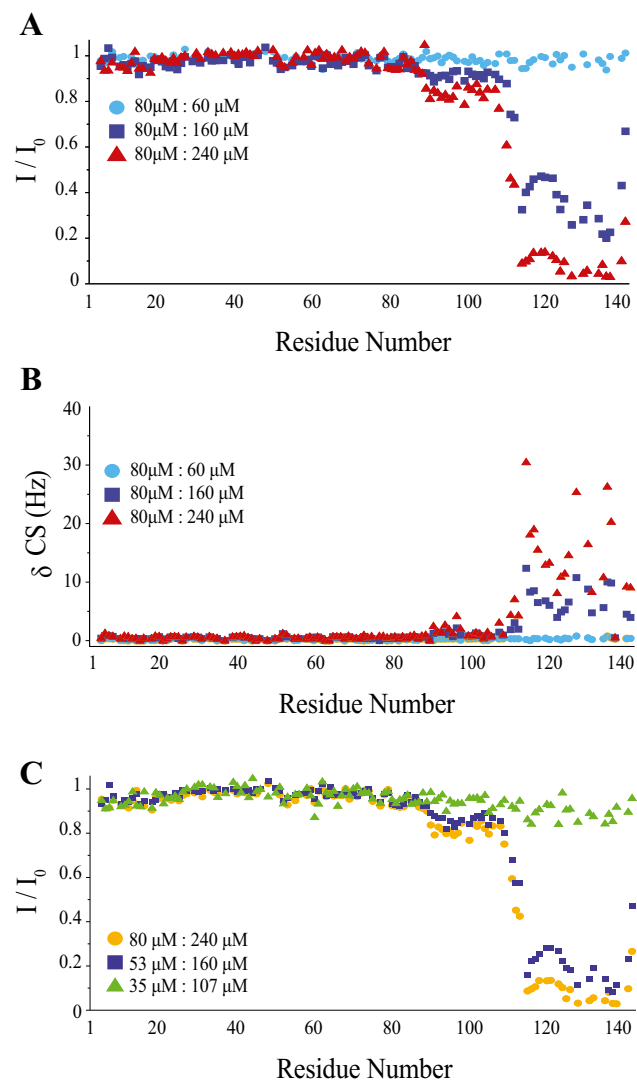


**Fig. S1.** Squalamine interacts directly with  $\alpha$ -synuclein at high concentrations. (A) Ratios of  $\alpha$ -synuclein HSQC peak heights in the presence of different concentrations of squalamine compared with free  $\alpha$ -synuclein. The sample contained 80  $\mu\text{M}$   $\alpha$ -synuclein, and three concentrations of squalamine were tested: 60  $\mu\text{M}$  (blue circles), 160  $\mu\text{M}$  (violet squares), and 240  $\mu\text{M}$  (red triangles). The buffer conditions were 20 mM imidazole (pH 6), 100 mM NaCl. (B) Changes in chemical shifts measured at a frequency of 600 MHz  $^1\text{H}$  resulting from squalamine addition compared with free  $\alpha$ -synuclein.  $\delta_{CS}$  was defined as  $\delta_{CS} = \sqrt{\delta_{CS}^2 + (\frac{\delta_H}{2})^2}$ , where  $\delta_N$  and  $\delta_H$  are the changes in resonance frequency (in hertz units) for  $^{15}\text{N}$  and  $^1\text{H}$ , respectively. The sample contained 80  $\mu\text{M}$   $\alpha$ -synuclein, and three concentrations of squalamine were tested: 80  $\mu\text{M}$  (blue circles), 160  $\mu\text{M}$  (violet squares), and 240  $\mu\text{M}$  (red triangles). (C) Ratios of  $\alpha$ -synuclein HSQC peak heights are shown for three samples at different concentrations with a fixed squalamine: $\alpha$ -synuclein ratio: 80  $\mu\text{M}$   $\alpha$ -synuclein and 240  $\mu\text{M}$  squalamine (yellow circles), 53  $\mu\text{M}$   $\alpha$ -synuclein and 160  $\mu\text{M}$  squalamine (dark blue squares), and 35  $\mu\text{M}$   $\alpha$ -synuclein and 107  $\mu\text{M}$  squalamine (green triangles).

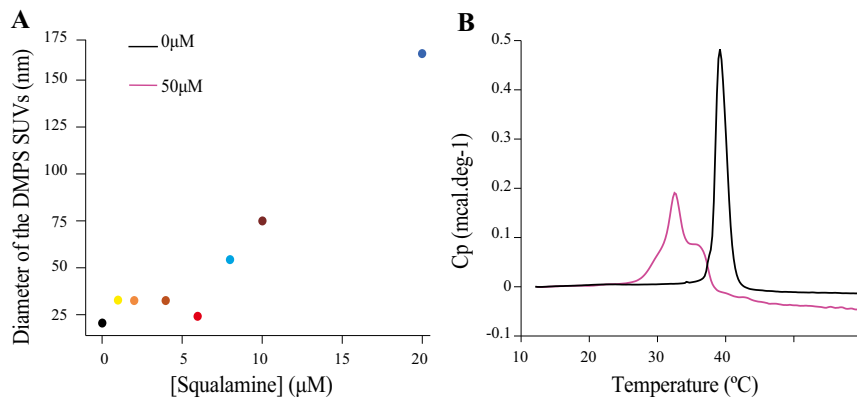


**Fig. S2.** Effect of squalamine on the size and the thermotropic properties of DMPS vesicles. (A) Change in the diameter of DMPS vesicles (100  $\mu\text{M}$ ) with increasing concentrations of squalamine measured by dynamic light scattering. (B) Differential scanning calorimetry trace of 500  $\mu\text{M}$  DMPS in the absence and presence of 50  $\mu\text{M}$  squalamine.

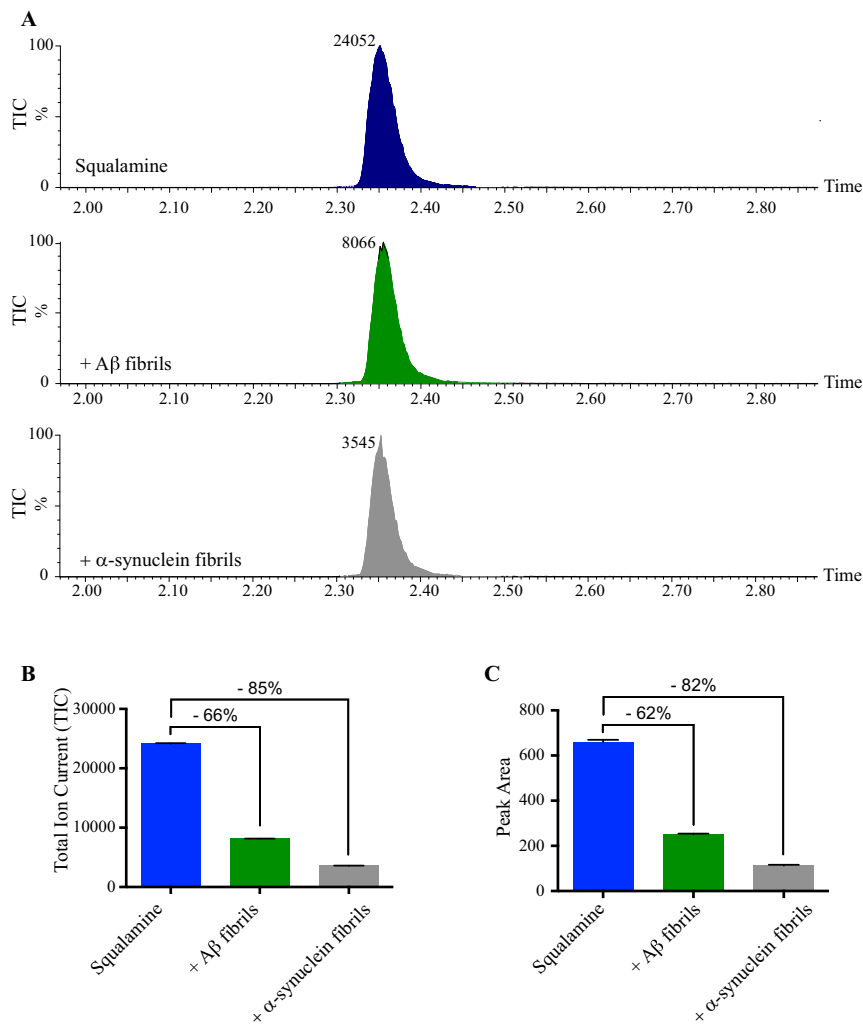


**Fig. S3.** Squalamine binding to A $\beta$  and  $\alpha$ -synuclein fibrils. (A) Total ion current (TIC) of 10  $\mu\text{M}$  squalamine (Top), TIC corresponding to the supernatant fraction after incubation with A $\beta$  (Middle), and  $\alpha$ -synuclein fibrils (Bottom), respectively. Experiments were carried out in triplicate and one representative experiment is shown. (B) TIC averaged over three independent experiments. (C) Peak area averaged over three independent experiments.  $\alpha$ -Synuclein and A $\beta$  fibrils were obtained as previously described (10, 13) and incubated overnight with 10  $\mu\text{M}$  squalamine.

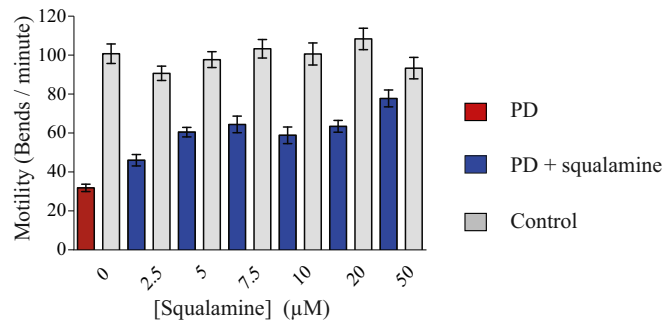


**Fig. 54.** Squalamine recovers the severe muscle paralysis associated with overexpression of  $\alpha$ -synuclein in PD worms (25). For experiments carried out in solid media, the protective effect is maximal at day 4 for 50  $\mu$ M squalamine. Red bars, PD; blue bars, treated PD; gray bars, controls. The plots show one representative of three experiments. Error bars represent the SEM.

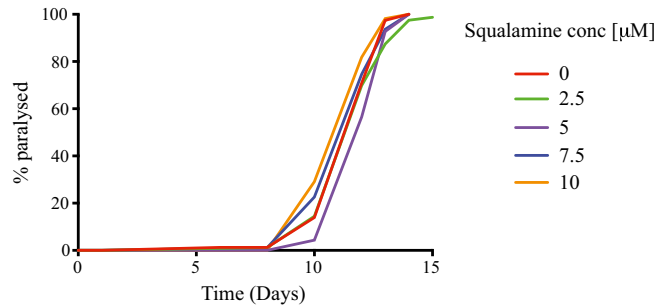
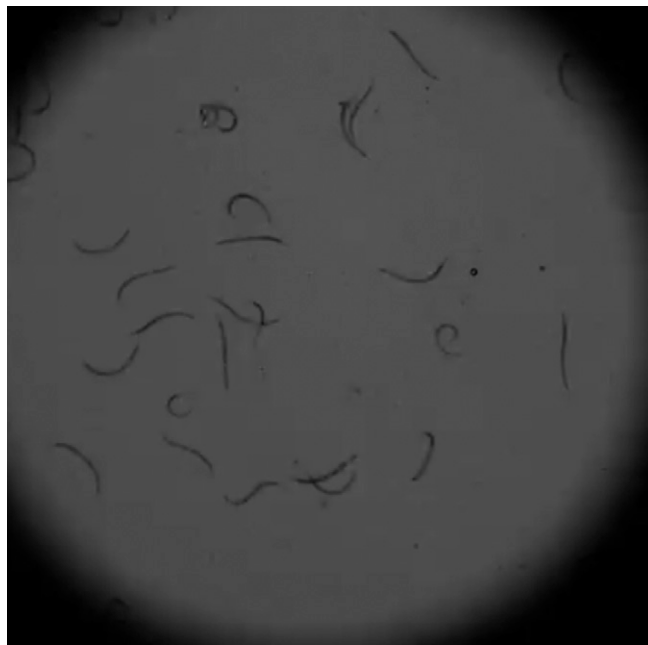
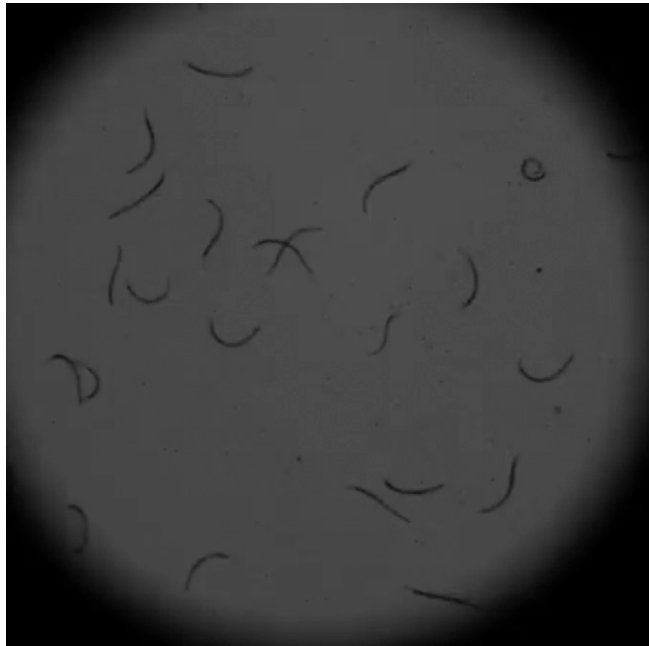


**Fig. 55.** Exposure to squalamine has less relevant effects on an A $\beta$  worm model. Squalamine administration at a concentration of 1–10  $\mu$ M had no significant protective effect (e.g., no decrease in the time of the onset of the paralysis) for an A $\beta$  worm model CL2006 (40). The plots show one representative of three experiments.



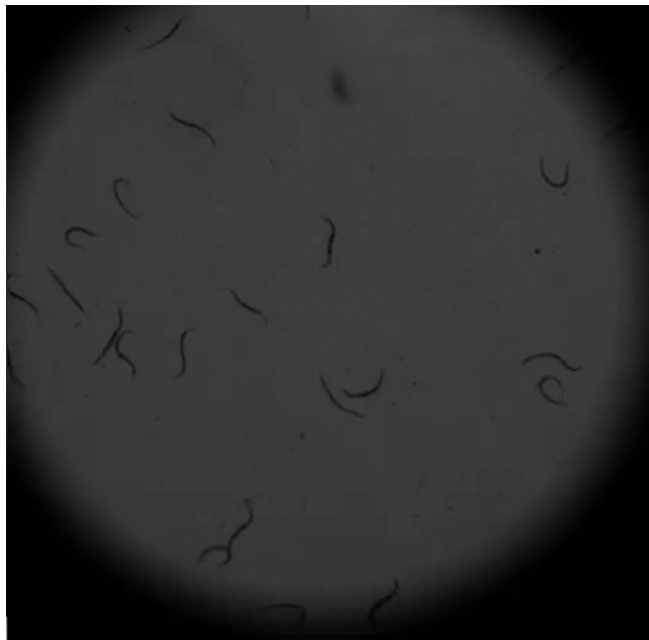
**Movie S1.** The mobility of untreated control worms at day 4 of adulthood.

[Movie S1](#)



**Movie S2.** The mobility of control worms treated with 50  $\mu$ M squalamine at day 4 of adulthood. Squalamine does not notably affect the motility of control worms.

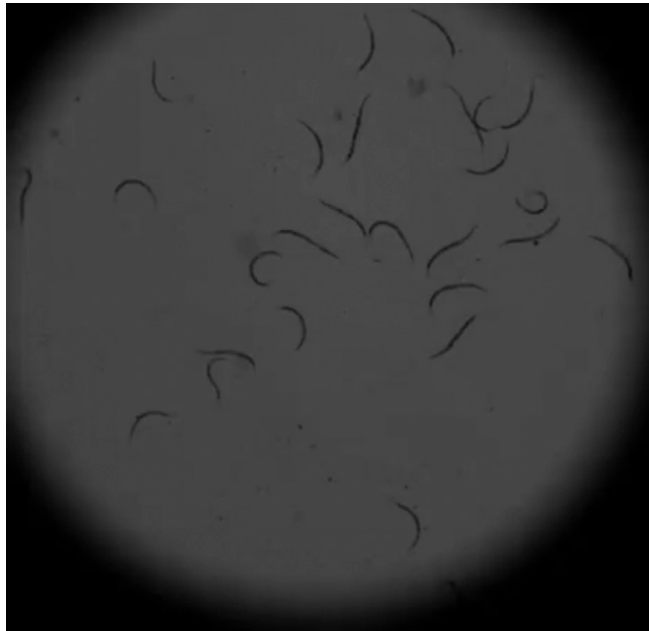
[Movie S2](#)



**Movie S3.** The mobility of untreated PD worms at day 4 of adulthood. It is clear the motility dysfunction is induced by  $\alpha$ -synuclein overexpression.

[Movie S3](#)





**Movie S4.** The mobility of treated PD worms at day 4 of adulthood. Squalamine greatly rescues the motility dysfunction induced by  $\alpha$ -synuclein over-expression.

[Movie S4](#)